

INSTRUMENTATION

Quantitation of Experimental Canine Infarct Size with Multipinhole and Rotating-Slanthole Tomography

Samuel E. Lewis, Ernest M. Stokely, Michael D. Devous, Sr., Frederick J. Bonte, L. Maximillian Buja, Robert W. Parkey, and James T. Willerson

University of Texas Southwestern Medical School, Dallas, Texas

Myocardial infarct size was estimated by three methods in a canine model, using Tc-99m pyrophosphate at 24 and 48 hr after coronary ligation. A gamma camera provided anterior, LAO, and lateral views, and was then fitted with multipinhole (MPH) and rotating-slanthole (RSH) collimators for tomographic studies, processed by computer to display frontal sections of the chest. Infarct weight was measured postmortem for comparison. All transmural infarcts were detected by all three imaging techniques. RSH tomography was superior to both MPH tomography and planar imaging for the detection of nontransmural infarction. Infarcts as small as 1.0 g were detected. Estimates of infarct volume measured from RSH slices showed an excellent correlation with infarct weight ($r = 0.89$) and were reproducible within acceptable limits. Estimates of infarct volume measured from MPH slices demonstrated a significantly poorer correlation with infarct weight ($r = 0.48$, $p < 0.01$). Both tomographic techniques may improve infarct visualization by suppressing overlying activity and increasing contrast between infarct and background, but both produce significant blur artifacts that hamper their utilization by inexperienced observers.

J Nucl Med 22: 1000-1005, 1981

The fraction of myocardial tissue involved in acute infarction has been shown to have important therapeutic and prognostic implications (1-4). Because of this, several diagnostic modalities have been used to measure infarct size noninvasively in man (5-21). Enzymatic, electrocardiographic, transmission computed tomographic (TCT), and scintigraphic techniques have all been applied with some success. Radionuclide methods are particularly attractive because of their suitability for use with patients in the intensive-care setting, and the potential to locate and size infarcts acceptably using an

infarct-avid agent such as technetium-99m stannous pyrophosphate (Tc-99m PPI).

Early attempts to size acute experimental infarcts using the greatest area subtended by the infarct on any of three planar images of the thoracic distribution of Tc-99m PPI gave good results for transmural anterior and anterolateral infarcts (11,16). However, posterior, inferior, septal, and nontransmural infarctions were difficult to quantify using this two-dimensional technique, especially small infarcts with nontransmural distributions. Indeed, approximately 3-5 g of necrotic tissue appeared to be the lower limit of consistently detectable infarction by planar imaging (22).

In a canine model, Stokely et al. have demonstrated that a four-pinhole longitudinal tomographic system extends the capability of Tc-99m PPI infarct sizing to include posterior and some nontransmural infarcts as

Received Mar. 26, 1981; revision accepted June 29, 1981.

For reprints contact: Samuel E. Lewis, MD, University of Texas, Health Science Center, Dept. of Radiology, 5323 Harry Hines Blvd., Dallas, TX 75235.

well as anterior lesions (23). However, significant practical limitations of the multipinhole approach were also identified.

The purpose of the present study was to compare the capabilities of two limited-angle longitudinal tomographic systems for the detection and sizing of small experimental myocardial infarcts in dogs.

MATERIALS AND METHODS

Twenty-one mongrel dogs were anesthetized with intravenous pentobarbital sodium. Through a left thoracotomy, one to three branches of the left anterior descending coronary artery were ligated at the mid level or below. The chest was closed and the animals allowed to recover. Twenty-four to 48 hr after occlusion, the animals were again lightly anesthetized with pentobarbital sodium and given 5–10 mCi Tc-99m PPI (2.5 mg) by direct venepuncture. Imaging was begun 1.5–2.5 hr later.

Planar images were acquired in anterior, 35° left anterior oblique (LAO), 70° left anterior oblique, and left lateral projections with a gamma camera equipped with a high-resolution collimator. Energy discrimination was provided by a 20% window centered on the 140-keV peak. Anterior projections were acquired to a density of 500,000 counts per image, and the other projections used the same imaging time. Digital data were stored in a computer system in a 128 × 128 × 10 format. This procedure is one our institution has used for routine clinical studies, and has been shown to provide an excellent compromise between image statistics and acquisition time.

Multipinhole and rotating-slanthole images were acquired in random order following the planar imaging.

A previously described four-pinhole collimator (23), based on the design of Vogel et al. (24) and constructed to fit a standard-field-of-view gamma camera, was used for multipinhole data acquisition. With the planar images as a guide, one million counts per image were collected in anterior and 45° LAO projections and stored in 128 × 128 × 8 format in a portable acquisition unit. This procedure represented a compromise between acquisition time and necessary statistics for backprojection reconstruction. The time for each of the multipinhole data sets was approximately the same as that for the multiple planar images. A weighted opposed-view backprojection algorithm was used to reconstruct five to nine frontal slices 1 cm apart. Three or four iterations of a deblurring algorithm based on the method of Tomitani and Tanaka (25) were applied to the backprojected reconstructions.

Rotating-slanthole images were acquired with a 25° high-resolution slanthole collimator mounted on a gamma camera, the detector being parallel to the ante-

rior chest wall in each of six angular projections separated by 60°. Images were acquired to a density of 200,000 counts per image and stored in 128 × 128 × 10 format in a computer system. This provided about the same total number of events, and required about the same time, as did the multipinhole series. A weighted opposed-view backprojection algorithm was used to reconstruct 12 slices 0.5 cm apart. Three iterations of a least-squares algorithm developed by Gottschalk et al. (26) were applied to the backprojected reconstructions.

SCINTIGRAPHIC INFARCT SIZING

Two-dimensional (2D) estimates of infarct size were obtained by computer-aided manual planimetry of the infarct area in each of the four planar projections (16). Reproducibility was tested by sizing the scintigrams blindly three to five times over a period of 2 wk. Scale-factor calibration was provided by two point sources separated by exactly 5 cm. The largest area in any projection was taken as the estimate of infarct area.

Tomographic infarct sizing from multipinhole data was performed by computer-aided manual planimetry of the Tc-99m PPI uptake in each reconstructed slice. Areas from each 1-cm slice were assumed to be 1 cm thick, and were added to give infarct volume (23). The planar images were available for review during the sizing procedure. A single point source at 14 cm was used to determine the x and y scale factors of the reconstructed images. The scale factor in each reconstructed slice was corrected to a constant 2.5 mm/pixel dimension using an interpolation algorithm. The average result of at least two estimates of infarct volume obtained on separate occasions was used for comparison with postmortem measurement of infarct weight.

Tomographic sizing from rotating-slanthole data was performed in similar fashion, with calibration of reconstructed images obtained by a point source at 24 cm and two point sources exactly 5 cm apart.

All scintigraphic estimates of infarct size were made without knowledge of the necropsy results.

POSTMORTEM DETERMINATION OF EXPERIMENTAL INFARCT SIZE

Following completion of the imaging studies, the animals were killed with large doses of pentobarbital sodium and the hearts removed. The hearts were sliced transversely into five sections, which were washed in saline and placed in a 1% solution of 2,5,3-triphenyl tetrazolium chloride (TTC) in phosphate buffer for 30 min or until the normal myocardium was stained (16). The sections were then fixed in phosphate-buffered formalin. The left-ventricular myocardium was weighed for each slice, and the unstained, infarcted portion of each slice was excised and weighed. Total infarct weight

TABLE 1. DETECTION OF MYOCARDIAL INFARCTION

Technique	All infarcts	Transmural	Nontransmural
Planar	18/21 (85.7%)	14/14 (100%)	4/7 (57.1%)
MPH	19/21 (90.5%)	14/14 (100%)	5/7 (71.4%)
RSH	21/21 (100%)	14/14 (100%)	7/7 (100%)

Abbreviations: MPH - multipinhole tomography; RSH - rotating-slanthole tomography.

was recorded as the sum of the infarct weights for all slices (16).

RESULTS

Infarcts were produced in all 21 animals and ranged in size from 1.0 to 23.0 g (mean = 10.1 ± 5.5 g). Fourteen infarcts were transmural, with a range of 7.1–23.0 g (mean = 12.9 ± 9.0 g). Seven infarcts were nontransmural with a range of 1.0–9.0 g (mean = 4.5 ± 3.1 g).

Table 1 compares the results of the three imaging techniques for detection of myocardial infarction. All 14 transmural infarcts were detected by planar imaging and were easily identified on the reconstructed slices produced by both tomographic systems. Among the nontransmural infarcts, however, only four of seven were detected by planar imaging and only five of seven by multipinhole imaging. These results are further characterized in Table 2.

Figure 1 shows the correlation between anatomical infarct weight and measurements of infarct area. The 2D estimates (when obtainable) demonstrated a correlation with postmortem measurements ($r = 0.72$) that was quite similar to that in our previous results for grouped transmural and nontransmural infarcts. However, five infarcts that were identified by planar imaging could not be reproducibly sized because of faint uptake and/or indistinct boundaries, and are not included in this correlation. These five ranged in size from 9.0 to 17.1 g (mean = 12.9 ± 2.7 g). Four of the five were transmural.

Figure 2 shows the correlation between anatomical infarct weight and infarct volume estimated from multipinhole data acquired in the anterior projection. The

TABLE 2. DETECTION OF NONTRANSMURAL INFARCTS

Infarct wt.	2D	MPH	RSH
1.0 g	—	+	+
2.5 g	+	+	+
2.7 g	+	+	+
3.2 g	—	—	+
4.3 g	—	—	+
8.5 g	+	+	+
9.0 g	+	+	+

r value of 0.48 ($p < 0.01$) is considerably poorer than in our previous results with the four-pinhole technique. This is probably due to the lower mean infarct weight and greater percentage of nontransmural infarctions in this series, and because in our earlier series the animals were killed immediately before imaging in order to simulate a gated acquisition. As in our previous study (23), the results from the 45° LAO projection were significantly different from those obtained in the anterior projection and showed a poorer correlation with postmortem infarct weight.

Figure 3 shows the correlation between postmortem infarct weight and rotating-slanthole estimates of infarct volume. The latter estimates ($r = 0.89$) were significantly different from multipinhole volume estimates ($r = 0.48$) at the $p < 0.05$ level (paired t -test).

Reproducibility for the 2D sizing estimates was calculated from at least three planimetric measurements of each planar image set. The coefficient of variation (CV) for the planimetric infarct area was calculated for each animal. Values ranged from 3.2–7.5% for those animals that were correlated with postmortem infarct weight. The CVs for the five animals that could not be reliably sized and were not correlated with infarct weight ranged from 25 to 50%. Reproducibility of the infarct-area determination in these five was significantly different from that in the other animals at the $p < 0.001$ level.

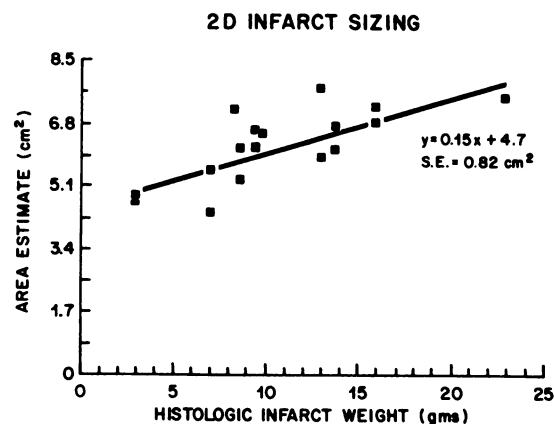


FIG. 1. Correlation ($r = 0.72$) between anatomical and scintigraphic infarct size using largest area in four standard Tc-PPI scintigrams (anterior 35° LAO, 70° LAO, left lateral) as the best estimator of infarct weight.

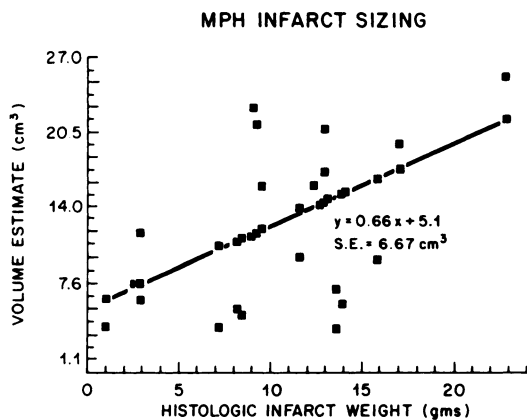


FIG. 2. Poor correlation ($r = 0.48$) between multipinhole tomographic estimates of infarct volume and postmortem infarct weight.

Reproducibility for the tomographic sizing estimates was evaluated by calculating the error between the first and second measurements of infarct volume. These errors were much smaller than the root-mean-square deviation from regression for both multipinhole and rotating-slanthole estimates. The regressions for the first and second sizings were not significantly different.

DISCUSSION

Measurements of infarct size in patients seem to have considerable predictive power concerning the immediate postevent hospital course. Page et al. have shown that serious complications of infarction can be anticipated when the size of an acute infarct, or the combined size of acute and chronic events in the same patient, equals 40% or more of the total left-ventricular muscle mass (1). The development of pump failure and cardiogenic shock are particularly devastating postinfarction complications. Serious ventricular arrhythmias, refractory to medical management, also seem related to infarct size (8). In addition, the segments of the left ventricle that are damaged by infarction appear to have further prognostic implications (27-29). Development of means to assess the amount of damaged myocardial tissue and to discover the location of such damage in the left ventricle will have an important bearing on the patient's medical management. It will be particularly important to monitor the effects of therapy directed at limiting infarct size.

Scintigraphic imaging with the infarct-avid Tc-99m PPI tracer has been shown to be a sensitive indicator of myocardial necrosis (30). Anatomical location of infarction by Tc-99m PPI also shows excellent correlation with pathologic findings (31). Recently developed methods to superimpose Tc-99m PPI images and radionuclide ventriculograms provide a dramatic means to correlate infarct location with segmental ventricular dysfunction (32). Two-dimensional estimates of infarct

size made from multiple planar images show good correlation with infarct weight for anterior and anterolateral transmural infarcts (16), but for nontransmural infarcts and nonanterior transmural infarcts, 2D size estimates correlate poorly with infarct weight. Attempts to extract tomographic information from orthogonal planar images using a model of the infarct cross section have shown some success (33,34), but have the disadvantage of requiring the arbitrary selection of the model to apply to a specific study.

Many of the problems associated with planar imaging for the detection, localization, and sizing of acute myocardial infarction can theoretically be obviated by the application of emission computed tomography (ECT). Commonly available techniques for performing single-photon ECT can be classified into rotational and limited-angle approaches. Rotating-detector or rotating-patient systems have been used by Budinger (35), Keyes (36), Singh (37), Burdine (38), and others to produce cross-sectional images of the myocardium with both infarct-avid and flow-distributed tracers. Such rotational techniques may add valuable information to that obtained from routine multiview planar images. In general, rotational systems are far superior to limited-angle techniques, because the projections must cover at least 180° for the accurate reconstruction of a cross section, and many projections within the angular coverage are needed to achieve a unique reconstruction (39). However, rotational systems do have some disadvantages for cardiovascular imaging. The current rotational systems force the detector to travel in a circular orbit, and since the thorax is not a cylinder, this results in increased detector-to-chest distances for the important anterior projections. In addition, these devices may be impractical in intensive-care settings. For cardiovascular imaging, limited-angle tomographic techniques have somewhat different problems. As noted earlier, their tomographic effect is limited by the angle subtended by the projections. The results also depend upon object geometry and

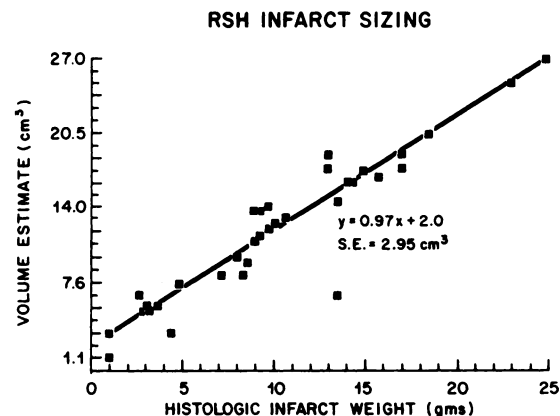


FIG. 3. Correlation ($r = 0.89$) between rotating-slanthole tomographic estimates of infarct volume and postmortem infarct weight.

relative orientation of the object to the detector. This may be used to advantage in myocardial imaging. Phantom studies have demonstrated that multipinhole tomography improves contrast in thallium-201 images if the detector can be positioned directly along, and orthogonal to, the long axis of the left ventricle (40). The results of clinical studies, however, have been mixed (41,42). For Tc-99m PPI infarct-avid imaging, Stokely et al. have shown that a four-pinhole system extends infarct sizing capability in experimental infarction to include posterior and nontransmural infarcts as small as 1.8 g (23). In our study, rotating-slanthole tomography was superior to MPH tomography and planar images in detecting infarction. Estimates of infarct volume obtained from the RSH reconstructions showed excellent correlation with infarct weight, and were acceptably reproducible. MPH sizing demonstrated a significantly poorer correlation with infarct weight, a correlation poorer than in our earlier results. This may be due to the smaller mean infarct size in the present study, the greater percentage of nontransmural infarcts, and the absence of gated acquisition.

The results of this study should be equally valid for comparisons between seven-pinhole and rotating-slanthole tomography when all images are acquired with a standard-field gamma camera. The fundamental limitation on reconstruction from limited angles is the lack of a complete set of Fourier coefficients (i.e., projections) because the total angle subtended by the projections falls short of the minimum 180° range necessary for accurate reconstruction (39). We used four pinholes rather than seven because this allowed the viewed volume to be moved closer to the camera crystal, thereby providing a wider range of viewing angles for each pinhole image. Simulation of an eight-pinhole system did not show significant improvement over the four-pinhole (23).

The extrapolation of animal results to man is often difficult, and this is certainly true for the current study. Clinically, the blur artifacts present in the tomographic reconstructions may result in an increased number of false-positive studies. Moreover, Tc-99m PPI images in dogs tend to have significantly better target-to-background ratios than analogous images obtained in critically ill patients. Since all of the animals in this study had acute infarction, we do not know whether the increased sensitivity for the detection of small infarcts achieved by limited-angle tomography is offset by a decreased specificity.

ACKNOWLEDGMENTS

The authors appreciate the expert technical assistance of Ms. Dorothy Gutekunst and Ms. Katie Wolf, who prepared the animal models used in this study. Ms. Tommie Hall provided valuable assistance in obtaining the scintigraphic images.

This work was supported in part by the NIH Ischemic Heart Disease SCOR Grant HL 17669.

REFERENCES

1. PAGE DL, CAULFIELD JB, KASTOR JA, et al: Myocardial changes associated with cardiogenic shock. *N Engl J Med* 285:133-137, 1971
2. ALONSO DR, SCHEIDT W, POST M, et al: Pathophysiology of cardiogenic shock. Quantification of myocardial necrosis: clinical, pathologic, and electrocardiographic correlations. *Circulation* 48:588-596, 1973
3. SOBEL BE: Infarct size, prognosis, and causal contiguity. *Circulation* 53:I-146-I-148, 1976
4. BOOR PJ, REYNOLDS ES: Myocardial infarct size: Clinicopathologic agreement and discordance. *Human Pathol* 8:685-695, 1977
5. ADAMS DF, HESSEL SJ, JUDY PF, et al: Computed tomography of the normal and infarcted myocardium. *Am J Roentgenol* 126:786-791, 1976
6. BERNINGER WH, REDINGTON RW, DOHERTY P, et al: Gated cardiac scanning: canine studies. *J Comput Assist Tomogr* 3:155-163, 1979
7. BUJA LM, PARKEY RW, STOKELY EM, et al: Pathophysiology of technetium-99m stannous pyrophosphate and thallium-201 scintigraphy of acute anterior myocardial infarcts in dogs. *J Clin Invest* 57:1508-1522, 1976
8. COX JR JR, ROBERTS R, AMBOS HD, et al: Relations between enzymatically estimated myocardial infarct size and early ventricular dysrhythmia. *Circulation* 53:1-150-1-155, 1976
9. GRAY WR, BUJA LM, HAGLER HK, et al: Computed tomography for localization and sizing of experimental acute myocardial infarcts. *Circulation* 58:497-504, 1978
10. HOLMAN BL, LESCH M, ZWEIMAN FG, et al: Detection and sizing of acute myocardial infarcts with 99m-Tc(Sn) tetracycline. *N Engl J Med* 291:159-163, 1974
11. BOTVINICK EH, SHAMES D, LAPPIN H, et al: Noninvasive quantitation of myocardial infarction with technetium 99m pyrophosphate. *Circulation* 52:909-915, 1975
12. KJEKSHUS JK, SOBEL BE: Depressed myocardial creatine phosphokinase activity following experimental myocardial infarction in rabbit. *Circ Res* 27:403-414, 1970
13. MAROKO PR, KJEKSHUS JK, SOBEL BE, et al: Factors influencing infarct size following experimental coronary artery occlusions. *Circulation* 43:67-82, 1971
14. MULLER JE, MAROKO PR, BRAUNWALD E: Evaluation of precordial electrocardiographic mapping as a means of assessing changes in myocardial ischemic injury. *Circulation* 52:16-27, 1975
15. MURRAY RG, PESHOCK RM, PARKEY RW, et al: ST isopotential precordial surface maps in patients with acute myocardial infarction. *J Electrocard* 12:55-64, 1979
16. STOKELY EM, BUJA LM, LEWIS SE, et al: Measurement of acute myocardial infarcts in dogs with 99mTc-stannous pyrophosphate scintigrams. *J Nucl Med* 17:1-5, 1976
17. SHELL WE, KJEKSHUS JK, SOBEL BE: Quantitative assessment of the extent of myocardial infarction in the conscious dog by means of analysis of serial changes in serum creatine phosphokinase activity. *J Clin Invest* 50:2614-2625, 1971
18. TENNANT R, WIGGERS CJ: The effect of coronary occlusion on myocardial contraction. *Am J Physiol* 112:351-361, 1935
19. THEROUX P, FRANKLIN D, ROSS J JR, et al: Regional myocardial function during acute coronary artery occlusion and its modification by pharmacologic agents in the dog. *Circ Res* 35:896-908, 1974
20. WACKERS FJT, BECKER AE, SAMSON G, et al: Location and size of acute transmural myocardial infarction estimated

- from thallium-201 scintiscans. *Circulation* 56:72-78, 1977
21. HENNING H, SCHELBERT HR, RIGHETTI A, et al: Dual myocardial imaging with technetium-99m pyrophosphate and thallium-201 for detecting, localizing, and sizing acute myocardial infarction. *Am J Cardiol* 40:147-155, 1977
 22. POLINER LR, BUJA LM, PARKEY RW, et al: Comparison of different noninvasive methods of infarct sizing during experimental myocardial infarction. *J Nucl Med* 18:517-523, 1977
 23. STOKELY EM, TIPTON DM, BUJA LM, et al: Quantitation of experimental canine infarct size using multipinhole single-photon tomography. *J Nucl Med* 22:55-61, 1981
 24. VOGEL RA, KIRCH DL, LEFREE MT, et al: A new method of emission tomography using compound collimation. In *Proceedings of the Fifth International Conference on Information Processing in Medical Imaging, Nashville, TN*. Oak Ridge, Oak Ridge National Laboratories, Biomedical Computing Technology Information Center, ORNL/BCTIC-1, 1977, pp 636-646
 25. TOMITANI T, TANAKA E: Three-dimensional reconstruction in longitudinal tomography by means of iterative approximation. In *Proceedings of the Fifth International Conference on Information Processing in Medical Imaging, Nashville, TN*. Oak Ridge, Oak Ridge National Laboratories, ORNL/BCTIC-2, 1977, pp 174-194
 26. GOTTSCHALK S, SMITH KA, WAKE RH: Comparison of seven pinhole and rotating slant tomography of a cardiac phantom. *J Nucl Med* 21:P27, 1980 (abst)
 27. OHSUZU F, BOUCHER CA, OSBAKKEN MD, et al: Contribution of segmental wall motion to ejection fraction in patients with acute myocardial infarction. *J Nucl Med* 21:P52, 1980 (abst)
 28. MILLER RR, OLSON HG, VISMARA LA, et al: Pump dysfunction after myocardial infarction: Importance of location, extent and pattern of abnormal left ventricular segmental contraction. *Am J Cardiol* 37:340-344, 1976
 29. STRAUSS H, AMBROS H, SOBEL BE, et al: Relationships between the site of infarction, infarct size, and mortality. *Am J Cardiol* 41:361, 1978 (abst)
 30. Parkey RW, Bonte FJ, Buja LM, et al., Eds: *Clinical Nuclear Cardiology*. New York, Appleton-Century-Crofts, 1979
 31. BUJA LM, POLINER LR, PARKEY RW, et al: Clinicopathologic findings in 52 patients studied by technetium-99m stannous pyrophosphate myocardial scintigraphy. *Circulation* 59:257-267, 1979
 32. CORBETT JR, LEWIS SE, DEHMER GJ, et al: Simultaneous display of gated technetium-99m stannous pyrophosphate and gated blood-pool scintigrams. *J Nucl Med* 22:671-677, 1981
 33. LEWIS MH, BUJA LM, SAFFER S, et al: Experimental infarct sizing using computer processing and a three-dimensional model. *Science* 197:167-169, 1977
 34. LEWIS MH, BUJA LM, PARKEY RW, et al: A computer-based scintigraphic method for sizing acute inferior myocardial infarcts. *Radiology* 136:439-442, 1980
 35. BUDINGER TF: Three-dimensional imaging of the myocardium with isotopes. In *Cardiovascular Imaging and Image Processing*. Harrison DC, Andler H, Miller HA, Eds. Palos Verdes, CA, Society of Photo-Optical Instrumentation Engineers, 1975, pp 263-271
 36. KEYES JW JR, LEONARD PF, BRODY SL, et al: Myocardial infarct quantification in the dog by single photon emission computed tomography. *Circulation* 58:227-232, 1978
 37. SINGH M, BERGGREN MJ, GUSTAFSON DE, et al: Emission-computed tomography and its application to imaging of acute myocardial infarction in intact dogs using Tc-99m pyrophosphate. *J Nucl Med* 20:50-56, 1979
 38. BURDINE JA, MURPHY PH, DEPUEY EG: Radionuclide computed tomography of the body using routine radiopharmaceuticals II. Clinical applications. *J Nucl Med* 20:108-114, 1979
 39. CHIU MY, BARRETT HH, SIMPSON RG, et al: Three-dimensional radiographic imaging with a restricted view angle. *J Opt Soc Am* 69:1323-1333, 1979
 40. WILLIAMS DL, RITCHIE JL, HARP GD, et al: In vivo simulation thallium-201 myocardial scintigraphy by seven-pinhole emission tomography. *J Nucl Med* 21:821-828, 1981
 41. VOGEL RA, KIRCH DL, LEFREE MT, et al: Thallium-201 myocardial perfusion scintigraphy: results of standard and multipinhole tomographic techniques. *Am J Cardiol* 43:787-793, 1979
 42. RITCHIE JL, WILLIAMS DL, CALDWELL JH, et al: Seven-pinhole emission tomography with thallium-201 in patients with prior myocardial infarction. *J Nucl Med* 22:107-112, 1981

**ANNUAL MEETING
SECTION ON NUCLEAR PHARMACY
AMERICAN PHARMACEUTICAL ASSOCIATION**

April 27-28, 1982

Las Vegas Convention Center

Las Vegas, Nevada

Announcement and Call for Abstracts

The Program Committee of the Section on Nuclear Pharmacy of APhA welcomes submission of original contributions on: radiopharmaceutical design, synthesis, biodistribution, kinetics, and quality control; clinical nuclear pharmacy; and economic aspects of nuclear pharmacy.

Official abstract forms and requests for information should be directed to:

Ronald L. Williams, S.N.P.
American Pharmaceutical Association
2215 Constitution Ave., N.W.
Washington, DC 20037
Tel: (202)628-4410

Deadline for receipt of abstracts is December 15, 1981.